IEEE Access
Multidisciplinary | Rapid Review | Open Access Journal

Received September 28, 2018, accepted October 16, 2018, date of publication October 29, 2018,
date of current version November 19, 2018.

Digital Object Identifier 10.1109/ACCESS.2018.2878101

Enhancing INS/UWB Integrated Position Estimation Using Federated EFIR Filtering

YUAN XU[1,2], (Member, IEEE), GUOHUI TIAN[1], (Member, IEEE), AND XIYUAN CHEN[3], (Senior Member, IEEE)

[1]School of Control Science and Engineering, Shandong University, Jinan 250061, China
[2]School of Electrical Engineering, University of Jinan, Jinan 250022, China
[3]School of Instrument Science and Engineering, Southeast University, Nanjing 210096, China

Corresponding authors: Guohui Tian (g.h.tian@sdu.edu.cn) and Xiyuan Chen (chxiyuan@seu.edu.cn)

This work was supported in part by the National Natural Science Foundation of China under Grant 61803175, Grant 61873064, and Grant 61773239, in part by the Shandong Provincial Natural Science Foundation, China, under Grant ZR2018LF010 and Grant ZR2017QF007, in part by a project of Shandong Province Higher Educational Science and Technology Program under Grant J18KA333, in part by the China Postdoctoral Science Foundation under Grant 2017M622204, and in part by the Doctoral Foundation of the University of Jinan under Grant XBS1503.

ABSTRACT In order to obtain accurate position information, a federated extended finite impulse response (EFIR) filter which includes sub-filters and main filter is proposed for inertial navigation system (INS)/ultrawideband (UWB)-integrated human positioning in this paper. Here, the EFIR filter is employed as the sub-filter, which is able to fusion the UWB- and INS-measured distances between the reference nodes and the target human. The main filter is used to provide the optimal INS position error estimation by fusing the outputs of the sub-filters, which is able to correct the INS position. The test results show that the performance of the proposed method is better than the traditional federated extended Kalman filter in position accuracy.

INDEX TERMS Indoor human positioning, inertial navigation system (INS), ultra wide band (UWB), tightly-coupled model, federated EFIR filtering.

I. INTRODUCTION

Nowadays, numerous applications need the position information of the person [1], especially in indoor environment [2]. Consequently, the topic of pedestrian navigation has attracted wide attention [3], [4]. However, it should be pointed out that although there are many topic on the human positioning for indoor environment, this topic is still the challenge.

In order to obtain the accurate position information, many approaches have been proposed. First of all, many localization technologies have been proposed. For example, an radio frequency identification (RFID) indoor positioning algorithm has been designed in [5]. A smartphone-based cooperative indoor localization with RFID technology is proposed in [6]. An active RFID trilateration and location fingerprinting based on RSSI for pedestrian navigation have been proposed in [7]. Meanwhile, a smartphone-based indoor localization with Bluetooth beacons is designed in [8]. The ZigBee-based underground localization algorithm is proposed in [9]. The Wi-Fi is also used by many approaches for the indoor localization. For example, a Wi-Fi-based indoor localization has been proposed in [10]. Moreover, a novel method for constructing a Wi-Fi positioning system with efficient manpower is designed in [11]. However, it should be pointed out that although the RFID and Wi-Fi are able to achieve the localization, their accuracy are not suitable for the high precision positioning and navigation requirements [3], [12]. In order to improve the accuracy, the Ultra Wide Band (UWB) is used to indoor positioning systems. For example, the UWB-based human positioning system is proposed in [13]. On the other hand, inertial navigation system (INS) has been used for indoor pedestrian navigation, for example in [14], pedestrian tracking with shoe-mounted inertial sensors has been designed. The advantage of the INS is that it does not rely auxiliary equipment such as the Reference nodes (RNs) in UWB. However, we have to say that the INS is not good at long-term navigation.

It should be emphasized that there are many shortcomings in the approaches mentioned above. In order to overcome the shortcomings of the localization technologies mentioned above, the integrated navigation has been proposed in [15]. For example, Zhuang *et al.* [16] proposed a PDR/INS/Wi-Fi integration for indoor tracking.

2169-3536 © 2018 IEEE. Translations and content mining are permitted for academic research only.
Personal use is also permitted, but republication/redistribution requires IEEE permission.
See http://www.ieee.org/publications_standards/publications/rights/index.html for more information.

A INS/UWB-integrated navigation has been proposed in [15]. To the integrated navigation, it includes three forms: loosely-coupled, tightly-coupled, and ultra-tightly-coupled integration [17]. The loosely-coupled integrated navigation is widely used since it is easy to achieve, however, its performance is limited by the requirements of the signal navigation method. For example, the UWB has to employ at least three RNs to complete the positioning independently. In order to overcome this problem and to further improve the accuracy, the tightly-coupled integrated navigation is proposed [18], [19]. For instance, [12] designs an accurate pedestrian indoor navigation by tightly coupling foot-mounted inertial measurement unit (IMU) and RFID measurements. And a tightly-coupled integration of Wi-Fi and MEMS sensors on handheld devices for indoor pedestrian navigation is proposed in [20]. In this model, the sensor data is input to the data fusion filter directly compared with the loosely-coupled integrated navigation.

On the other hand, it should be pointed out that the data fusion filter also plays an important roles on the improvement of the accuracy. To the filtering algorithm, Kalman filter (KF)-based filter, such as extended KF (EKF) [21], iterated EKF (IEKF) [22], Unscented KF (UKF) [23], has been proved to be effective for optimal estimation. However, the KF-based filter has to get accurate noise statistics for the good performance [24]. In practice, this condition is difficult to be guaranteed. In order to get good performance, the finite impulse response (FIR) filters [25] fusing most recent data has been proposed. For example, a FIR filtering for accurate RFID-based self-Localization is designed in [26]. In [3], an improving UFIR filter-based adaptive INS/UWB-integrated human tracking is proposed.

In [4] and [27], we proposed a distributed EKF-based approaches for the INS/UWB-integrated indoor tracking, which employ the EKF and IEKF as the sub-filter and the main filter to fuse the outputs of the sub-filter. It should be pointed out that although the EKF is able to improve the accuracy of the data fusion filter, its performance is not robustness. In order to improve the robustness of the data fusion filter, we present an improving federated extended finite impulse response (EFIR) filter for INS/UWB-integrated human positioning in this paper. In this model, we employ EFIR filter as the sub-filter for the data fuse in each wireless channel, and the distances measured by the UWB and that values measured by the IMU are both sent to the EFIR filter. Then, the main filter works with the output of the sub-EFIR filter and output the estimation of the INS position error. The optimal estimation of the navigation solution is calculated by the INS position and the filter output. A real indoor test is implemented for evaluating the performance of the proposed filtering method.

The remainder of the paper is organized as follows: Section II presents the principle of the tightly-coupled integrated human positioning and the design of the federated EFIR filter. Section III discuss the real test and its results. Section IV gives the conclusions.

II. THE SCHEME OF FEDERATED EFIR FILTER-BASED TIGHTLY-COUPLED INTEGRATED HUMAN POSITIONING

In this section, firstly, the scheme of the tightly-coupled integrated human positioning used in this paper will be reviewed. Then, the federated extended finite impulse response (EFIR) filter will be designed based on tightly-coupled integrated scheme.

A. TIGHTLY-COUPLED INTEGRATED HUMAN POSITIONING

Fig. 1 pictures the structure of the tightly-coupled INS/UWB model for human positioning used in this work, which is also used in [4], [15], and [28]. Thus, we briefly review the tightly integrated navigation model. The INS/UWB-integrated system includes INS and UWB systems. To the UWB system, it contains one blind node (BN) and N reference nodes (RNs), here, N is the number of the RNs. To the INS, it employs the inertial measurement unit (IMU), which fixed on the foot of the target human. The federated EFIR filter will be employed as the data fusion filter of the integrated system, which uses the distances between the RNs and BN measured by the UWB (denote as $d^{(UWB)_{(i)}}, i \in (1, N)$) and that values measured by the INS (denote as $d^{(INS)_{(i)}}, i \in (1, N)$). The federated EFIR filter is able to estimate the optimal INS position error, which will be used to correct the INS position measured by the IMU. The design of the federated EFIR filter will be present in the next section.

B. THE FEDERATED EFIR FILTER FOR THE TIGHTLY-COUPLED INTEGRATED HUMAN POSITIONING

In this section, the federated EFIR filter based on the tightly-coupled scheme which is proposed in the Section II-A will be designed in detail. The block diagram of the federated EFIR filter is pictured in Fig. 2. To the scheme of the federated EFIR filter, it includes N sub-filters and one main filter. In this federated mode, the sub-filter is employing to provide the local estimation of INS position error by fusing the $d^{(UWB)_{(i)}}$ and the $d^{(UWB)_{(i)}}$ based on the *ith* channel. Then, the main filter is used to provide the final output of the data fusion filter, which fuses the local estimations of the sub-filters.

Based on the structure of the federated EFIR filter, the state equation and the measurement equation will be designed as following. To the *ith* sub-filter, the state equation used by the sub-filter at the time index q can be written as follows

$$\underbrace{\begin{bmatrix} \delta P^{(i)}_{E,q} \\ \delta V^{(i)}_{E,q} \\ \delta P^{(i)}_{N,q} \\ \delta V^{(i)}_{N,q} \end{bmatrix}}_{x^{(i)}_{q|q-1}} = \underbrace{\begin{bmatrix} 1 & \Delta T & 0 & 0 \\ 0 & 1 & 0 & 0 \\ 0 & 0 & 1 & \Delta T \\ 0 & 0 & 0 & 1 \end{bmatrix}}_{A^{(i)}_{q-1}} \underbrace{\begin{bmatrix} \delta P^{(i)}_{E,q-1} \\ \delta V^{(i)}_{E,q-1} \\ \delta P^{(i)}_{N,q-1} \\ \delta V^{(i)}_{N,q-1} \end{bmatrix}}_{x^{(i)}_{q-1}} + \mathbf{w}^{(i)}_{q-1}, \tag{1}$$

where $\left(\delta P^{(i)}_{E,q}, \delta P^{(i)}_{N,q}\right)$ represent the INS position errors derived from the *ith* sub-filter in east and north directions at

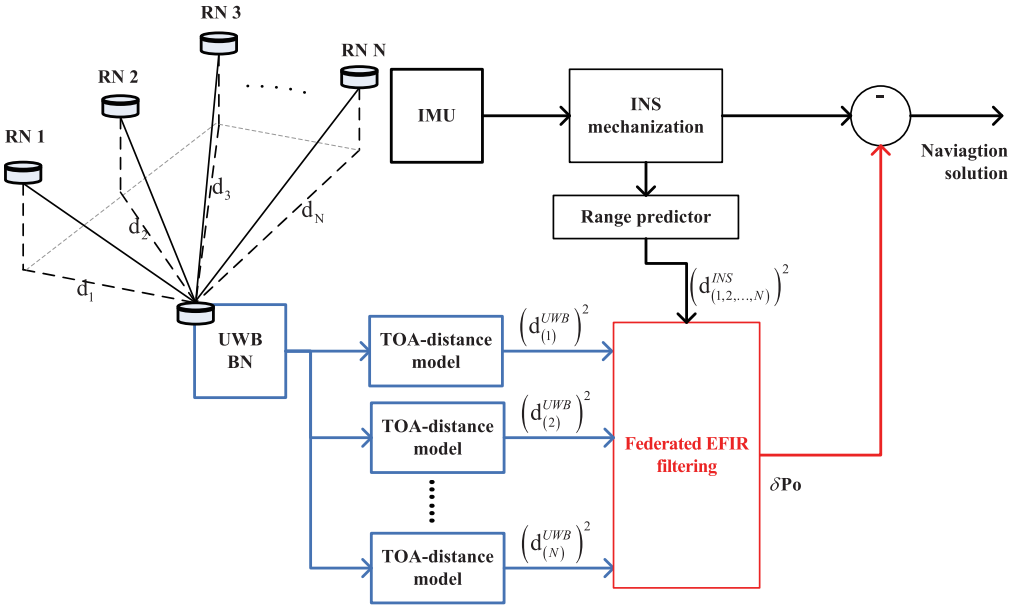

FIGURE 1. The block diagram of the tightly-coupled INS/UWB-integrated scheme.

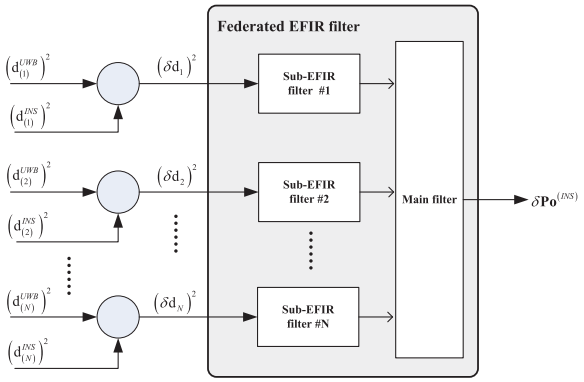

FIGURE 2. The block diagram of the federated EFIR filter.

time index q respectively. $\left(\delta V_{E,q}^{(i)}, \delta V_{N,q}^{(i)}\right)$ represent the INS velocity errors derived from the *ith* sub-filter in east and north directions at time index q respectively. ΔT is the sample time, and the $\mathbf{w}_q^{(i)}$ is the system noise, its covariance is $\mathbf{Q}_q^{(i)}$. The $x_q^{(i)}$ denotes the state vector for the *ith* sub-filter at time index q, and the $A_q^{(i)}$ denotes system matrix for the *ith* sub-filter at time index q.

The measurement equation for the *ith* sub-filter can be written as Eq. (2), as shown at the bottom of the next page, where $\left(P_E^{(i)}, P_N^{(i)}\right)$ is the position of the *ith* RN in east direction and north direction. $\eta_q^{(i)}$ is the measurement noise for the *ith* sub-filter at time index q, its covariance is $\mathbf{R}_q^{(i)}$. It should be emphasized that the detailed deducing can be find in [15] and [29].

With the system (1) and (2), the data fusion filter can be designed. To the data fusion filter, one of the famous example is the Kalman filter (KF) [12], [15]. It should be pointed out that the KF has to employ the accurate noise statics [30] to obtain good performance of the estimation. However, one can find it is hard to get accurate noise statics in real test. On the other hand, the current filtering algorithm is dominated by centralized filtering, which is not good at the fault detection compared with the distributed filter. In this paper, in order to obtain the good performance, we use the EFIR filter as the sub-filter. With the system (1) and (2), the pseudo code of the EFIR filter is listed in Algorithm 1.

With the sub-filter, the main filter can work to fusion the outputs of the sub-filter, then, the final output of the data fusion filter can be calculated as Eq. (3).

$$\hat{x}_q = P_q\left(\left(P_q^{(1)}\right)^{-1}\hat{x}_q^{(1)} + \left(P_q^{(2)}\right)^{-1}\hat{x}_q^{(2)} + \left(P_q^{(3)}\right)^{-1}\hat{x}_q^{(3)} + \ldots + \left(P_q^{(N)}\right)^{-1}\hat{x}_q^{(N)}\right), \quad (3)$$

$$P_q = \left(\left(P_q^{(1)}\right)^{-1} + \left(P_q^{(2)}\right)^{-1} + \left(P_q^{(3)}\right)^{-1} + \ldots + \left(P_q^{(N)}\right)^{-1}\right)^{-1}, \quad (4)$$

The pseudo code of the federal EFIR filter is listed in Algorithm 2. From the algorithm, one can find that the federal EFIR filter firstly employ the Algorithm 1 to complete the local estimation (lines 4–15). Then, the main filter fuses the outputs of the sub-filters (lines 16–17).

III. TEST

In this section, a real test will be done to verify the performance of the proposed federal EFIR filter. Firstly, the setting of the test will be designed. Then, the performances of the

Algorithm 1 EFIR Filter for the *ith* Channel

Data: $Y_q^{(i)}, M^E, N^E, Q^{(i)}, R^{(i)}$
Result: $\hat{x}_q^{(i)}, \hat{P}_{qq}^{(i)}$

begin
  for $q = N^E : \infty$ **do**
    $p = q - N^E + 1, \quad r = p + M^E - 1$
    for $qq = r + 1 : q$ **do**
      $\tilde{x}_{qq|qq-1}^{(i)} = A_{qq}^{(i)} \tilde{x}_{qq-1}^{(i)} + w_{qq}^{(i)}$
      $P_{qq|qq-1}^{(i)} = A_{qq-1}^{(i)} P_{qq-1}^{(i)} \left(A_{qq-1}^{(i)}\right)^T + Q^{(i)}$
      $G_{qq}^{(i)} = \left[H_{qq}^T H_q + \left(A_{qq} G_{qq-1} A_{qq}^T\right)^{-1}\right]^{-1}$
      $K_{qq}^{(i)} = G_{qq}^{(i)} \left(H_{qq}^{(i)}\right)^T$
      $\tilde{x}_{qq}^{(i)} = \tilde{x}_{qq-1}^{(i)} + K_q^{(i)} (Y_{qq}^{(i)} - h\left(\tilde{x}_{qq|qq-1}^{(i)}\right))$
      $P_{qq}^{(i)} = \left(I - K_{qq}^{(i)} H_{qq}^{(i)}\right) P_{qq|qq-1}^{(i)} \left(I - K_{qq}^{(i)} H_{qq}^{(i)}\right)^T + K_{qq}^{(i)} R^{(i)} \left(K_{qq}^{(i)}\right)^T$
    end for
    $\hat{x}_{qq}^{(i)} = \tilde{x}_{qq}^{(i)}$
    $\hat{P}_{qq}^{(i)} = P_{qq}^{(i)}$
  end for
end
† M^E represents the error state vector size
† N^E represents the horizon size
† $H_{qq}^{(i)} = \frac{\partial h\left(x_{qq|qq-1}^{(i)}\right)}{\partial x_{qq|qq-1}^{(i)}}$

Algorithm 2 Federal EFIR Filter

Data: $Y_q^{(i)}, M^E, N^E, Q^{(i)}, R^{(i)}$
Result: $\hat{x}_q, \hat{P}_q$

begin
  for $q = N^E : \infty$ **do**
    $p = q - N^E + 1, \quad r = p + M^E - 1$
    for $i = 1 : N$ **do**
      for $qq = r + 1 : q$ **do**
        $\tilde{x}_{qq|qq-1}^{(i)} = A_{qq}^{(i)} \tilde{x}_{qq-1}^{(i)} + w_{qq}^{(i)}$
        $P_{qq|qq-1}^{(i)} = A_{qq-1}^{(i)} P_{qq-1}^{(i)} \left(A_{qq-1}^{(i)}\right)^T + Q^{(i)}$
        $G_{qq}^{(i)} = \left[H_{qq}^T H_q + \left(A_{qq} G_{qq-1} A_{qq}^T\right)^{-1}\right]^{-1}$
        $K_{qq}^{(i)} = G_{qq}^{(i)} \left(H_{qq}^{(i)}\right)^T$
        $\tilde{x}_{qq}^{(i)} = \tilde{x}_{qq-1}^{(i)} + K_q^{(i)} (Y_{qq}^{(i)} - h\left(\tilde{x}_{qq|qq-1}^{(i)}\right))$
        $P_{qq}^{(i)} = \left(I - K_{qq}^{(i)} H_{qq}^{(i)}\right) P_{qq|qq-1}^{(i)} \left(I - K_{qq}^{(i)} H_{qq}^{(i)}\right)^T + K_{qq}^{(i)} R^{(i)} \left(K_{qq}^{(i)}\right)^T$
      end for
      $\hat{x}_{qq}^{(i)} = \tilde{x}_{qq}^{(i)}$
      $\hat{P}_{qq}^{(i)} = P_{qq}^{(i)}$
    end for
    $\hat{x}_q = P_q \left(\left(P_q^{(1)}\right)^{-1} \hat{x}_q^{(1)} + \left(P_q^{(2)}\right)^{-1} \hat{x}_q^{(2)} + \left(P_q^{(3)}\right)^{-1} \hat{x}_q^{(3)} + \ldots + \left(P_q^{(N)}\right)^{-1} \hat{x}_q^{(N)}\right)$
    $P_q = \left(\left(P_q^{(1)}\right)^{-1} + \left(P_q^{(2)}\right)^{-1} + \left(P_q^{(3)}\right)^{-1} + \ldots + \left(P_q^{(N)}\right)^{-1}\right)^{-1}$
    for $i = 1 : N$ **do**
      $\tilde{x}_q^{(i)} = \hat{x}_q$
      $P_q^{(i)} = P_q$
    end for
  end for
end
† $H_{qq}^{(i)} = \frac{\partial h\left(x_{qq|qq-1}^{(i)}\right)}{\partial x_{qq|qq-1}^{(i)}}$

federal Kalman filter and the proposed federal EFIR filter will be compared.

A. SETTING

In this subsection, the setting of the real test will be discussed. In order to show the performance of the proposed federal EFIR filter, the real test has been done in the mechanical experiment building, University of Jinan. In this paper, both the UWB system and INS are used for the test. The real test environment is pictured in Fig. 3. To the UWB system, in this

$$\underbrace{\left[\delta\left(d_q^{(i)}\right)^2\right]}_{Y_q^{(i)}} = \left[\left(d_{(i),q}^{INS}\right)^2 - \left(d_{(i),q}^{UWB}\right)^2\right]$$
$$= \underbrace{2\left(P_{E,q}^{(i)} - P_E^{(i)}\right)\delta P_{E,q}^{(i)} + 2\left(P_{N,q}^{(i)} - P_N^{(i)}\right)\delta P_{N,q}^{(i)} - \left(\left(\delta P_{E,q}^{(i)}\right)^2 + \left(\delta P_{N,q}^{(i)}\right)^2\right)}_{h\left(x_{q|q-1}^{(i)}\right)} + \underbrace{\left[\eta_{d_{(i),q}}\right]}_{\eta_q^{(i)}}, \tag{2}$$

FIGURE 3. The real test environment.

test, we employ four UWB RNs and one UWB BN. We assign four IDs (A0, A1, A2, A3) to the UWB RNs. Here, the UWB RNs are fixed on the known position, meanwhile, the UWB BN is fixed on the target human. The UWB system used in this paper is able to measure the distance between the UWB RNs and the UWB BN which is shown in Fig. 1. The size of the UWB RNs is $45 \times 45 \times 85$ mm (*length* $\times$ *width* $\times$ *height*), and it weighs 34.2 g, the size of the UWB BN is $45.4 \times 45.4 \times 33.5$ mm (*length* $\times$ *width* $\times$ *height*), and it weighs 42.3 g. To the INS, the inertial measurement unit (IMU) is used to measure the INS position, which can be used to computed the distance between the UWB RNs and the target human. The IMU is fixed on the foot of the target human. Its size is $48 \times 28 \times 13$ mm (*length* $\times$ *width* $\times$ *height*), and it weighs 20 g, the performance of the IMU used in this paper are summarized in Table 1. In the test, the Visual software based on C++ is used to collect the sensor data, then, the software will periodically store sensor data.

TABLE 1. The performance of the IMU used in this paper.

	Accelerometers	Gyroscopes	Magnetometers
Axes	3	3	3
Full Scale	$\pm$ 5 g	$\pm$ 300 deg/s	$\pm$ 8 Gauss
ADC Bit	16	16	12
Update rate	1-100 Hz	1-100 Hz	1-100 Hz

Meanwhile, in order to provide the reference velocity of the target human, we employ a reference system, which includes the encoder. Here, we firstly build the mapping $f()$ of the distance from the start point L_p and reference coordinations $\left(P_E^{(r)}, P_N^{(r)}\right)$. Then, the L_p is measured by the encoder, and the $\left(P_E^{(r)}, P_N^{(r)}\right)$ can be computed via the mapping $f()$. Moreover, in order to obtain the sensor data, the computer is used. In this work, to the system (1) and (2), we can obtain that $M^E = 4$, a and we set $N^E = 5$ and the sample time $\Delta T = 0.03$ s. Here, it should be pointed out that the setting method of N^E in Algorithms 1 and 2 can be find in [15]. The target human used in the test is pictured in Fig. 4. The setting for the EKF and the EFIR filter is listed in Table 2.

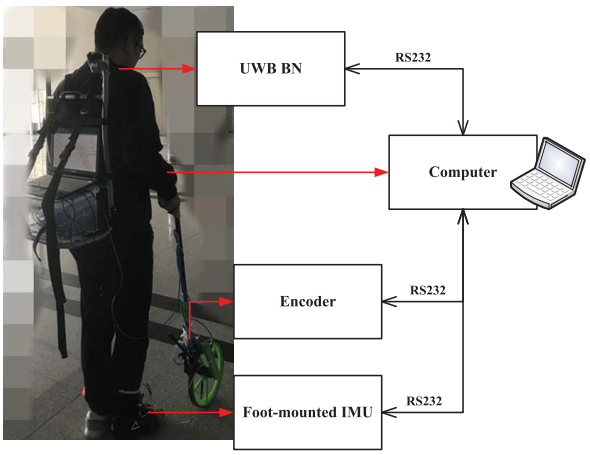

FIGURE 4. The target human used in the test.

TABLE 2. The setting for the EKF and the EFIR filter.

	EKF		EFIR filter	
	$\mathbf{Q}^{(i)}$	$\mathbf{R}^{(i)}$	M^E	N^E
Value	$3 \times 10^{-3.5} \times \mathbf{I}_{4\times 4}$	2	4	5

B. PERFORMANCES OF THE INS AND UWB

Fig. 5 pictures the reference path and the trajectories produced by the INS and UWB. And the position errors in

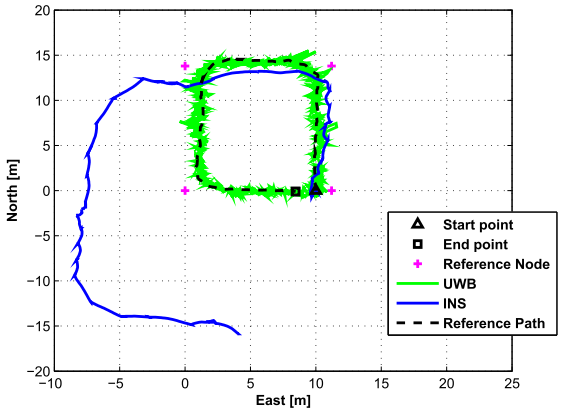

FIGURE 5. The reference path and the trajectories measured from the INS with ZUPT and UWB.

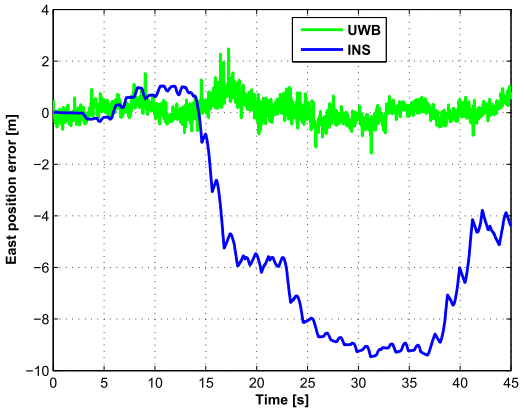

FIGURE 6. The east position errors estimated by the UWB and INS.

east and north estimated by the INS and UWB are shown in Figs. 6 and 7. Here, the INS solution is corrected by the zero velocity updating (ZUPT), thus, we denotes this model as INS+ZUPT model. Moreover, the UWB solution is computed by the least square method, and we denote this model as UWB. From the figure, we can see that the INS solution is close to the reference path in the initial stage of the test. However, the position error gets bigger at the end of the test due to the error accumulation. Consequently, we can get the conclusion that INS is not suitable for long-time working. To the UWB, it can be seen obviously that the UWB position error does not appear error accumulation compared with the INS solution. The position error of UWB is random. The mean square error (MSE) of the position in east and north directions produced by the INS and UWB are listed in Table 3. From the table, it can be seen that the localization accuracy of UWB is better than that of INS.

C. PERFORMANCE OF THE PROPOSED FEDERATED EFIR FILTER

In this subsection, the performances of the UWB, federal EKF, and federal EFIR filter will be compared using two test with the groups of parameters listed in Table 4.

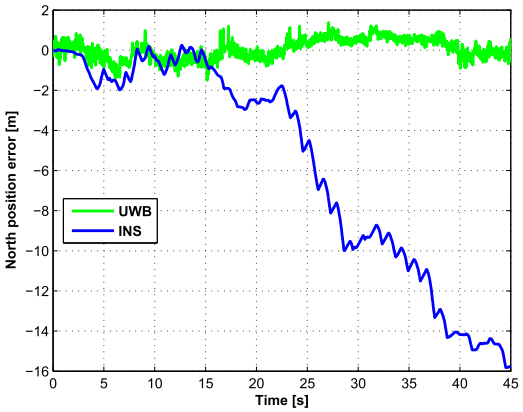

FIGURE 7. The north position errors estimated by the UWB and INS.

TABLE 3. MSE of the position in east and north directions produced by the INS and UWB.

Method	RMSE (m)	
	East	North
INS	5.98	7.79
UWB	0.42	0.51

TABLE 4. Two groups of parameters for the test.

	$\mathbf{x}_0$	$\mathbf{P}_0$	$\mathbf{Q}$	$\mathbf{R}$
Test 1	$\mathbf{0}_{4\times1}$	$\mathbf{I}_{4\times4}$	$0.3\times\mathbf{I}_{4\times4}$	$2\times10^{2.5}$
Test 2	$\mathbf{0}_{4\times1}$	$\mathbf{I}_{4\times4}$	$10^{-4.5}\times\mathbf{I}_{4\times4}$	1×10^{-1}

TABLE 5. RMSE of the position in east and north directions produced by the UWB, the federated EKF, and the federated EFIR filter (Test 1).

Method	RMSE (m)	
	East	North
UWB	0.42	0.51
Federated EKF	0.37	0.43
Federated EFIR filter	0.36	0.45

D. COMPARISON OF LOCALIZATION ERRORS – TEST 1

In this subsection, we do the test with the Test 1 of parameters (listed in Table 4). The reference path and the trajectories estimated by the INS, UWB, federated EKF, and federated EFIR filter are shown in Fig. 8. The east and north position errors estimated by the UWB, the federated EKF, and the federated EFIR filter are shown in Figs. 9 and 10. The root mean square error (RMSE) of the position in east and north directions produced by the UWB, the federated EKF, and the federated EFIR filter are listed in Table 5. From the figures and the table, one can find easily that the both the federated EKF, and federated EFIR filter are able to reduce the INS position and give the optimal human position estimation. The performances of the federated EKF and federated EFIR filter are similar.

E. COMPARISON OF LOCALIZATION ERRORS – TEST 2

In this subsection, we do the test again with the Test 2 of parameters (listed in Table 4). The reference path and the

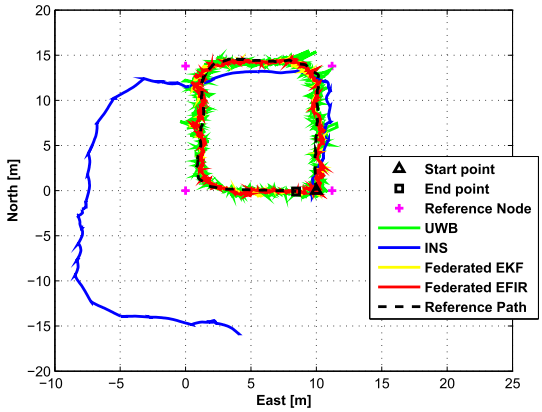

FIGURE 8. The reference path and the trajectories estimated by the INS, UWB, federated EKF, and federated EFIR filter (Test 1).

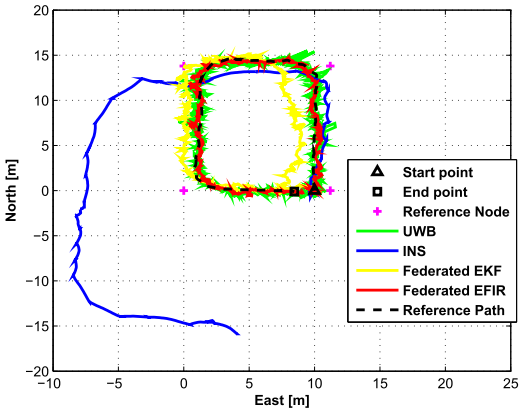

FIGURE 11. The reference path and the trajectories estimated by the INS, UWB, federated EKF, and federated EFIR filter (Test 2).

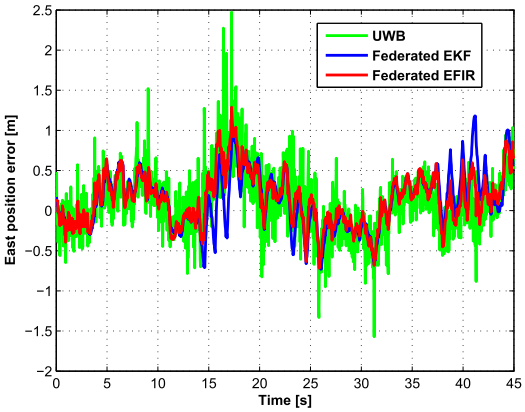

FIGURE 9. The east position errors estimated by the UWB, federated EKF, and federated EFIR filter (Test 1).

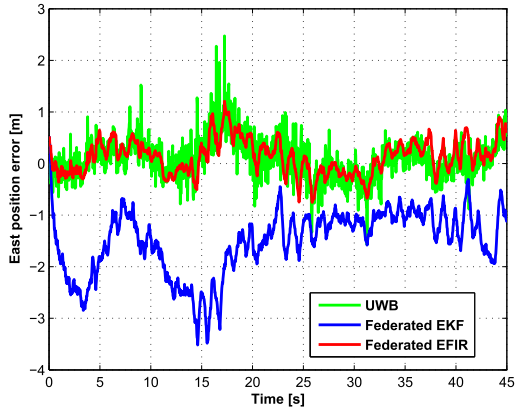

FIGURE 12. The east position errors estimated by the UWB, federated EKF, and federated EFIR filter (Test 2).

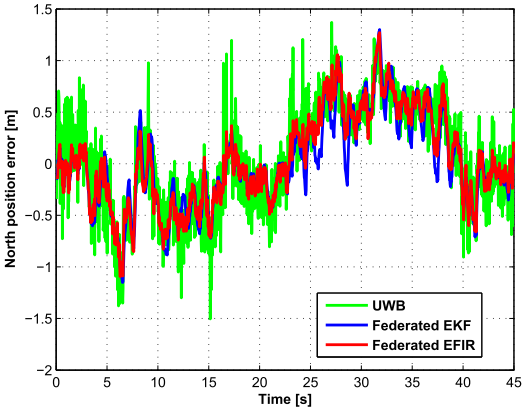

FIGURE 10. The north position errors estimated by the UWB, federated EKF, and federated EFIR filter (Test 1).

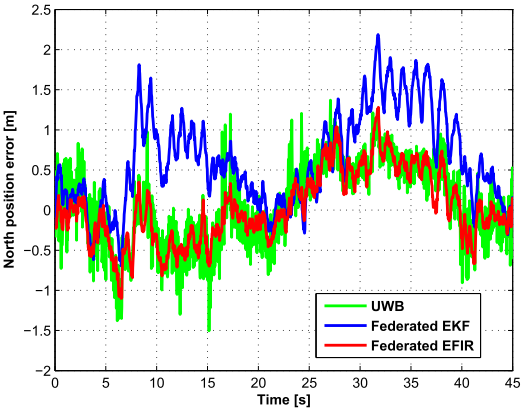

FIGURE 13. The north position errors estimated by the UWB, federated EKF, and federated EFIR filter (Test 2).

trajectories estimated by the INS, UWB, federated EKF, and federated EFIR filter are shown in Fig. 11. The east and north position errors estimated by the UWB, the federated EKF, and the federated EFIR filter are shown in Figs. 12 and 13. The cumulative error distribution function (CDF) is shown in Fig. 14. The position error used in Fig. 14 can be computed by the following.

$$Position\ error = \left|P_{E,q} - P^r_{E,q}\right| + \left|P_{N,q} - P^r_{N,q}\right|. \quad (5)$$

where $(P_{E,q}, P_{N,q})$ are the positions estimated by the filters in east direction and north direction, $(P_{E,q}, P_{N,q})$ are the reference positions in east direction and north direction.

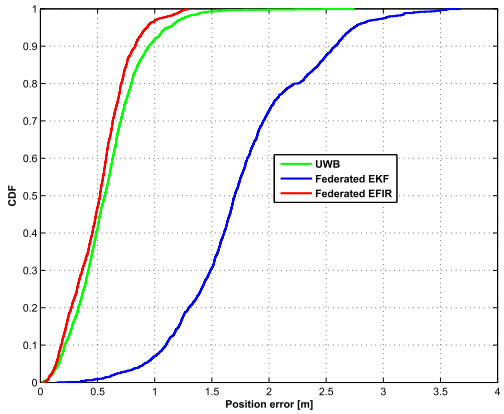

FIGURE 14. The CDF estimated by the UWB, federated EKF, and federated EFIR (Test 2).

TABLE 6. RMSE of the position in east and north directions produced by the UWB, the federated EKF, and the federated EFIR (Test 2).

Method	RMSE (m)	
	East	North
UWB	0.42	0.51
Federated EKF	1.64	0.86
Federated EFIR	0.36	0.45

The RMSE of the position in east and north directions produced by the UWB, the federated EKF, and the federated EFIR filter are listed in Table 6. From the figures and the table, one can find that the federated EKF is diverged. Compared with the federated EKF, the federated EFIR filter shows its robustness. In test 2, the federated EFIR filter is effective to reduce the INS position and give the optimal human position estimation.

IV. CONCLUSION

In this work, a federated EFIR filter and its application to the INS/UWB integrated human positioning have been proposed. The federated EFIR filter employs the sub-filter to fusion the UWB- and INS-measured distances between the RNs and the target human. Then, the main filter of the federated EFIR filter works with the outputs of the sub-EFIR filter and outputs the estimation of the INS position error. The optimal navigation solution will be calculated by the INS position and the output of the federated EFIR filter. Moreover, a real test has been done to verify the performance of the proposed federated EFIR filter. The test results show that the performance of the proposed method is better than the traditional federated EKF in position accuracy. Meanwhile, the federal EFIR filter shows its better robustness than the traditional federated EKF. In the future work, the missing data for the data fusion filter will be considered.

REFERENCES

[1] M. G. Puyol, D. Bobkov, P. Robertson, and T. Jost, "Pedestrian simultaneous localization and mapping in multistory buildings using inertial sensors," *IEEE Trans. Intell. Transp. Syst.*, vol. 15, no. 4, pp. 1714–1727, Aug. 2014.
[2] J. Jiao, F. Li, Z. Deng, and W. Ma, "A smartphone camera-based indoor positioning algorithm of crowded scenarios with the assistance of deep CNN," *Sensors*, vol. 17, no. 4, p. 704, Apr. 2017.
[3] Y. Xu, C. K. Ahn, Y. S. Shmaliy, X. Chen, and Y. Li, "Adaptive robust INS/UWB-integrated human tracking using UFIR filter bank," *Measurement*, vol. 123, pp. 1–7, Jul. 2018.
[4] Y. Xu, G. Tian, and X. Chen, "Performance enhancement for INS/UWB integrated indoor tracking using distributed iterated extended Kalman filter," in *Proc. Ubiquitous Positioning Indoor Navigat. Location-Based Services (UPINLBS)*, Apr. 2018, p. 15.
[5] H. Xu, Y. Ding, P. Li, R. Wang, and Y. Li, "An RFID indoor positioning algorithm based on Bayesian probability and K-nearest neighbor," *Sensors*, vol. 17, no. 8, p. 1806, 2017.
[6] F. Seco and A. R. Jiménez, "Smartphone-based cooperative indoor localization with RFID technology," *Sensors*, vol. 18, no. 1, p. 266, Jan. 2018.
[7] Q. Fu and G. Retscher, "Active RFID trilateration and location fingerprinting based on RSSI for pedestrian navigation," *J. Navigat.*, vol. 62, no. 2, pp. 323–340, Feb. 2009.
[8] Y. Zhuang, J. Yang, Y. Li, L. Qi, and N. El-Sheimy, "Smartphone-based indoor localization with Bluetooth low energy beacons," *Sensors*, vol. 16, no. 5, p. 596, Apr. 2016.
[9] Z. B. Zhang, X.-L. Xu, and L. L. Yan, "Underground localization algorithm of wireless sensor network based on ZigBee," *J. China Coal Soc.*, vol. 34, no. 1, pp. 125–128, Jan. 2009.
[10] N. Hernández, M. Ocaña, J. M. Alonso, and E. Kim, "Continuous space estimation: Increasing WiFi-based indoor localization resolution without increasing the site-survey effort," *Sensors*, vol. 17, no. 1, p. 147, Jan. 2017.
[11] Y. Du, D. Yang, and C. Xiu, "A novel method for constructing a WiFi positioning system with efficient manpower," *Sensors*, vol. 15, no. 4, pp. 8358–8381, Apr. 2015.
[12] A. R. J. Ruiz, F. S. Granja, J. C. P. Honorato, and J. I. G. Rosas, "Accurate pedestrian indoor navigation by tightly coupling foot-mounted IMU and RFID measurements," *IEEE Trans. Instrum. Meas.*, vol. 61, no. 1, pp. 178–189, Jan. 2011.
[13] Y. Xu, Y. S. Shmaliy, Y. Li, and X. Chen, "UWB-based indoor human localization with time-delayed data using EFIR filtering," *IEEE Access*, vol. 5, pp. 16676–16683, Aug. 2017.
[14] E. Foxlin, "Pedestrian tracking with shoe-mounted inertial sensors," *IEEE Comput. Graph. Appl.*, vol. 25, no. 6, pp. 38–46, Nov. 2005.
[15] Y. Xu, H. R. Karimi, Y. Li, F. Zhou, and L. Bu, "Real-time accurate pedestrian tracking using extended finite impulse response filter bank for tightly coupling recent inertial navigation system and ultra-wideband measurements," *Proc. Inst. Mech. Eng. I, J. Syst. Control Eng.*, vol. 232, no. 4, pp. 464–472, 2018.
[16] Y. Zhuang, H. Lan, Y. Li, and N. El-Sheimy, "PDR/INS/WiFi integration based on handheld devices for indoor pedestrian navigation," *Micromachines*, vol. 6, pp. 793–812, Jun. 2015.
[17] B. Cui, X. Chen, Y. Xu, H. Huang, and X. Liu, "Performance analysis of improved iterated cubature Kalman filter and its application to GNSS/INS," *ISA Trans.*, vol. 66, pp. 460–468, Jan. 2017.
[18] G. Xia and G. Wang, "INS/GNSS tightly-coupled integration using quaternion-based AUPF for USV," *Sensors*, vol. 16, no. 8, p. 1215, Aug. 2016.
[19] Z. Li, H. Zhang, Q. Zhou, and H. Che, "An adaptive low-cost INS/GNSS tightly-coupled integration architecture based on redundant measurement noise covariance estimation," *Sensors*, vol. 17, no. 9, p. 2032, Sep. 2017.
[20] Y. Zhuang and N. El-Sheimy, "Tightly-coupled integration of WiFi and MEMS sensors on handheld devices for indoor pedestrian navigation," *IEEE Sensors J.*, vol. 16, no. 1, pp. 224–234, Jan. 2015.
[21] T. B. Karamat, R. G. Lins, S. N. Givigi, and A. Noureldin, "Novel EKF-based vision/inertial system integration for improved navigation," *IEEE Trans. Instrum. Meas.*, vol. 67, no. 1, pp. 116–125, Jan. 2018.
[22] Y. Xu, X. Chen, and Q. Li, "Adaptive iterated extended Kalman filter and its application to autonomous integrated navigation for indoor robot," *Sci. World J.*, vol. 2014, no. 8, Aug. 2014, Art. no. 138548.
[23] J. Kong, X. Mao, and S. Li, "BDS/GPS dual systems positioning based on the modified SR-UKF algorithm," *Sensors*, vol. 16, no. 5, p. 635, May 2016.
[24] S. Zhao, Y. S. Shmaliy, C. K. Ahn, and F. Liu, "Adaptive-horizon iterative UFIR filtering algorithm with applications," *IEEE Trans. Ind. Electron.*, vol. 65, no. 8, pp. 6393–6402, Aug. 2018.
[25] S. Zhao, Y. S. Shmaliy, P. Shi, and C. K. Ahn, "Fusion Kalman/UFIR filter for state estimation with uncertain parameters and noise statistics," *IEEE Trans. Ind. Electron.*, vol. 64, no. 4, pp. 3075–3083, Apr. 2017.

[26] J. J. Pomarico-Franquiz and Y. S. Shmaliy, "Accurate self-localization in RFID tag information grids using FIR filtering," *IEEE Trans. Ind. Informat.*, vol. 10, no. 2, pp. 1317–1326, May 2014.
[27] Y. Xu, X.-Y. Chen, B.-B. Cui, and B. Wang, "Distributed unbiased tightly-coupled INS/UWB human localization via federated EKF," *J. Chin. Inertial Technol.*, vol. 25, no. 1, pp. 81–85, Jan. 2017.
[28] Y. Xu, X.-Y. Chen, and Q. H. Li, "Unbiased tightly-coupled INS/WSN integrated navigation based on extended Kalman filter," *J. Chin. Inertial Technol.*, vol. 20, no. 3, pp. 292–295, Jun. 2012.
[29] Y. Xu, X. Chen, J. Cheng, Q. Zhao, and Y. Wang, "Improving tightly-coupled model for indoor pedestrian navigation using foot-mounted IMU and UWB measurements," in *Proc. Instrum. Meas. Technol. Conf.*, May 2016, pp. 1–5.
[30] Y. S. Shmaliy, F. Lehmann, S. Zhao, and C. K. Ahn, "Comparing robustness of the Kalman, H∞, and UFIR filters," *IEEE Trans. Signal Process.*, vol. 66, no. 13, pp. 3447–3458, Jul. 2018.

YUAN XU (M'16) received the B.S. degree in automation from Shandong Polytechnic University in 2007, the M.S. degree in detection technology and automation device from Shandong Polytechnic University in 2010, and the Ph.D. degree in instrument science from Southeast University in 2014. He is currently a Post-Doctoral Researcher with the School of Control Science and Engineering, Shandong University. He is also a Lecturer with the School of Electrical Engineering, University of Jinan, Jinan, China. His research interests include integrated navigation and robust filtering.

GUOHUI TIAN (M'12) was born in Hejian, China, in 1969. He received the B.S. degree from the Department of Mathematics, Shandong University, Jinan, China, in 1990, the M.S. degree from the Department of Automation, Shandong University of Technology, Jinan, in 1993, and the Ph.D. degree from the School of Automation, Northeastern University, Shenyang, China, in 1997. He was a Post-Doctoral Researcher with the School of Mechanical Engineering, Shandong University, from 1999 to 2001, and a Visiting Professor with the Graduate School of Engineering, The University of Tokyo, Japan, from 2003 to 2005. He was with Shandong University as a Lecturer from 1997 to 1998 and an Associate Professor from 1998 to 2002. He is currently a Professor with the School of Control Science and Engineering, Shandong University. His research interests include service robot, intelligent space, cloud robotics, and brain-inspired intelligent robotics. And he is also the Vice Director of the Intelligence Robot Specialized Committee of the Chinese Association for Artificial Intelligence, the Vice Director of the Intelligent Manufacturing System Specialized Committee of the Chinese Association for Automation, and the member of the IEEE Robotics and Automation Society.

XIYUAN CHEN (M'08–SM'13) received the B.S. degree in mechanical engineering from the Lanzhou University of Technology, China, in 1990, the M.Sc. degree in mechanical engineering from the Hefei University of Technology, China, in 1995, and the Ph.D. degree in precision instrument and mechanical engineering from Southeast University, China, in 1998. He is currently a Professor with the School of Instrument Science and Engineering, Southeast University, China. His research interests include inertial navigation and integrated measurement.